IL NUOVO CIMENTO Vol. 35 C, N. 5 Settembre-Ottobre 2012
DOI 10.1393/ncc/i2012-11304-8

Communications: SIF Congress 2011

Measurement of the $Z \to \tau\tau$ cross-section in the semileptonic channel in pp collisions at $\sqrt{s} = 7\,\text{TeV}$ with the ATLAS detector

S. M. Consonni(*)

Dipartimento di Fisica, Università di Milano - via Celoria 16, 20134 Milano, Italy
INFN, Sezione di Milano - via Celoria 16, 20134 Milano, Italy

ricevuto il 30 Dicembre 2011; approvato il 26 Febbraio 2012
pubblicato online il 6 Settembre 2012

Summary. — Tau leptons play a fundamental role in the physics program of experiments at the LHC, since they are an important signature of Higgs boson production and SUSY. The Standard Model processes $W \to \tau\nu$ and $Z \to \tau\tau$ are standard candles for the assessment of the detector performance in identifying hadronically decaying tau leptons. The $Z \to \tau\tau$ cross-section was measured at ATLAS in pp collisions at $\sqrt{s} = 7\,\text{TeV}$ with the data sample collected in 2010, corresponding to $36\,\text{pb}^{-1}$, demonstrating the capabilities of ATLAS to perform measurements in tau channels. The measurement in the semileptonic channel is presented.

PACS 13.38.Dg – Decays of Z bosons.
PACS 13.85.Qk – Inclusive production with identified leptons, photons, or other nonhadronic particles.

1. – Introduction

The production of the Z boson and its decay to τ leptons is a benchmark process for physics with τ leptons at ATLAS.

Tau leptons are the charged third-family leptons, they are characterised by a large mass of $1776.82 \pm 0.16\,\text{MeV}$ and a short lifetime of $290.6 \pm 1.0\,\text{fs}$ [1]. The short lifetime implies that only the τ leptons decay products can actually be detected in an experimental apparatus such as that of ATLAS. The large mass allows then the τ lepton to have both leptonic and hadronic decays. Hadronic decays in particular can be 1-prong, that is the final state contains one charged hadron, or 3-prong.

But the τ leptons large mass is first of all one of the characteristics that makes them interesting for the search of new physics phenomena at the LHC: within the Standard Model (SM) the Higgs boson is expected to have larger couplings to massive particles,

(*) E-mail: sofia.consonni@mi.infn.it

which makes decays to tau leptons an attractive channel especially for a low mass Higgs boson. Moreover Higgs to τ pairs decays can be strongly enhanced with respect to SM couplings in large regions of parameter space within the Minimal Supersymmetric Standard Model (MSSM).

Besides this, in the MSSM framework charged Higgs bosons $H^{\pm}$ are predicted, for which the $H \to \tau\nu$ channel provides a unique signature and cascades containing τ leptons are present within Supersymmetric scenarios.

$Z \to \tau\tau$ and $W \to \tau\nu$ decays are important background processes in these searches and their production cross-sections need to be measured precisely. Studies of $Z \to \tau\tau$ processes at the LHC centre-of-mass energies are also interesting in their own right, complementing the measurements of the Z boson through the electron and muon decay modes. Finally, measuring the cross-section of a well-known Standard Model process involving τ leptons is highly important for the commissioning and validation of τ identification techniques, which will be crucial for fully exploiting the ATLAS experiment's potential in searches for new physics involving τ leptons.

The $Z \to \tau\tau$ cross-section was measured at ATLAS using four different final states in pp collisions at a centre-of-mass energy of $\sqrt{s} = 7\,\text{TeV}$ recorded with the ATLAS detector [2] at the LHC [3]. A full description of results can be found in ref. [4]. In this paper only the semileptonic decay modes $Z \to \tau\tau \to \mu + \text{hadrons} + 3\nu$ ($\tau_\mu\tau_h$) and $Z \to \tau\tau \to e + \text{hadrons} + 3\nu$ ($\tau_e\tau_h$) with branching fractions of $(22.50 \pm 0.09)\%$ and $(23.13 \pm 0.09)\%$, respectively [1] will be described. These modes offer a large branching fractions and imply many advantages such as the possibility to use single lepton triggers to select the events. The cross-section measurement in this channel in particular allows for a global check of the comprehension of analyses involving hadronically decaying τ leptons.

2. – The ATLAS detector

The ATLAS detector [2] is a multi-purpose apparatus operating at the LHC, designed to study a range of physics processes as wide as possible. ATLAS consists of several layers of subdetectors, from the interaction point outwards, the inner detector tracking system, the calorimeters, and the muon system([1]).

The inner detector is immersed in a 2 T magnetic field generated by the central solenoid. It is designed to provide high-precision tracking information which allows to measure the momentum of charged particles as well as provide information about their identity.

The calorimeters measure the energy of the particles by completely absorbing them. They are divided into an electromagnetic compartment, dedicated specifically to the measurement of electrons and photons, and a hadronic compartment, dedicated to the measurement of hadrons.

Muons are very penetrating particles, and therefore traverse the calorimeters without being absorbed. They are measured in the muon spectrometer, that relies on the

([1]) ATLAS uses a right-handed coordinate system with its origin at the nominal interaction point (IP) in the center of the detector and the z-axis along the beam pipe. The x-axis points from the IP to the center of the LHC ring, and the y-axis points upward. Cylindrical coordinates (r, ϕ) are used in the transverse plane, ϕ being the azimuthal angle around the beam pipe. The pseudorapidity is defined in terms of the polar angle θ as $\eta = -\ln\tan(\theta/2)$. The distance ΔR in the $\eta - \phi$ space is defined as $\Delta R = \sqrt{(\Delta\eta)^2 + (\Delta\phi)^2}$.

deflection of muons as they pass through the magnetic field of the large superconducting air-core toroid magnets.

The ATLAS detector has a three-level trigger system that acts as an event filter as well, in order to keep the rate of data going to mass storage sustainable.

3. – Data and Monte Carlo samples

The data sample used in this analysis corresponds to a total integrated luminosity of about $36\,\text{pb}^{-1}$, recorded with stable beam conditions and a fully operational detector in 2010.

Events are selected using either single lepton triggers with thresholds based on the transverse momentum (p_T) or transverse energy (E_T) of the muon or electron candidate, respectively. For the $\tau_\mu\tau_h$ final state, single muon triggers requiring $p_T > 10$–$13\,\text{GeV}$, depending on the run period, are used. For the $\tau_e\tau_h$ final state, a single electron trigger requiring $E_T > 15\,\text{GeV}$ is used. The thresholds level is fixed by a tradeoff between the sustainability of the rate at the EF level and the need of having a good kinematic acceptance for the soft electrons and muons from τ leptons decays. The efficiencies of the used triggers are determined from data using the so-called "tag-and-probe method", applied to $Z \to \mu\mu$, $Z \to ee$ and $W \to e\nu$ events, respectively.

The signal and background Monte Carlo (MC) samples used for this study are generated at $\sqrt{s} = 7\,\text{TeV}$ with the default ATLAS MC10 tune [5] and passed through a full detector simulation based on the GEANT4 program [6, 7]. More details on the samples used can be found in ref. [4].

4. – Cross-section calculation

The measurement of the cross-sections is obtained using the formula

$$\sigma(Z \to \tau\tau) \times B = \frac{N_{\text{obs}} - N_{\text{bkg}}}{A_Z \cdot C_Z \cdot \mathcal{L}}, \tag{1}$$

where N_{obs} is the number of observed events in data, N_{bkg} is the number of estimated background events, B is the branching fraction for the channel considered and $\mathcal{L}$ denotes the integrated luminosity for the final state of interest. C_Z is the correction factor that accounts for the efficiency of triggering, reconstructing and identifying the $Z \to \tau\tau$ events within the fiducial regions, defined by the full kinematic requirements applied to select the $Z \to \tau\tau$ events and summarised in sect. **5**.

The C_Z factor is determined as the ratio between the number of events passing the entire analysis selection after full detector simulation and the number of events in the fiducial region at generator level. The correction by the C_Z factor only provides the cross-section within the fiducial region of each measurement which is independent of the extrapolation procedure to the full phase space, and therefore is less affected by theoretical uncertainties in the modeling of the Z boson production.

The acceptance factor A_Z allows the extrapolation of σ^{fid} to the total cross-section, defined by eq. (1). The A_Z factor is determined from Monte Carlo as the ratio of events at generator level whose $\tau\tau$ invariant mass, before final state radiation, lies within the mass window [66, 116] GeV, and the number of events at generator level that fall within the fiducial regions defined above.

5. – Selection of $Z \to \tau\tau$ candidates

The selection of $Z \to \tau\tau$ events is based first of all on an event preselection, which allows to select events with a well-reconstructed primary vertex and to reject events with jets or τ candidates caused by out-of-time cosmic-rays, beam-halo events or known noise effects in the calorimeters.

Then events characterized by the presence of an isolated lepton([2]) and a hadronic τ decay([3]) are considered. Hadronic τ decays produce highly collimated jets in the detector consisting of an odd number of charged hadrons and additional calorimetric energy deposits from possible π^0 decay products. Finally, missing energy is expected from the neutrinos produced in the τ decays.

This implies the invariant mass of the system cannot be reconstructed trivially. In the context of this analysis the visible mass, defined as the invariant mass of the visible τ decay products only, is used.

5·1. *Reconstructed physics objects.* – A description of the reconstructed physics objects used in this analysis can be found in ref. [4].

Muons, electrons and taus are required to satisfy moderate transverse momentum/ energy thresholds, in order to have both a good kinematic acceptance and to select objects in a kinematic region where efficiencies are well known. Furthermore muons are required to lie in the pseudorapidity region where full trigger coverage is available, whereas electrons and taus are accepted in the full region where tracking information is available, excluding the calorimeter region where the performance is poor due to the presence of detector services. Additionally, muons, electrons and taus are required to satisfy tight reconstruction and identification criteria. In particular, tau candidates are identified against jets and electrons using variables describing the $\eta - \phi$ width of the candididate as well as particle identification information both from tracking and calorimetry. Leptons finally are required to be isolated, using variables that quantify the additional activity in a cone around the candidate.

Since neutrinos are emitted in the τ decays, genuine missing transverse momentum (E_T^{miss}) is expected in signal events.

5·2. *Event selection.* – After a basic topology selection it is necessary to apply additional requirements in order to suppress the contribution of background events in the selected sample. In particular multijet events can fake the $Z \to \tau\tau \to \ell\tau_{\text{h}}$ signature with a lepton, which can be either a fake from a jet or a genuine lepton from a semileptonic hadron decay, and a fake τ candidate from a jet. The multijet background is already strongly suppressed at this stage by the lepton isolation requirement and τ identification. Nevertheless τ candidates are further required to have unitary charge and 1 or 3 associated tracks. Events due to $W \to l\nu$ and $W \to \tau\nu$ typically enter the sample thanks to the genuine lepton and a fake τ candidate due to an additional jet in the event.

For signal events the E_T^{miss} vector is expected to fall in the azimuthal range spanned by the decay products, while in $W \to \ell\nu$ + jets events it will tend to point outside of the angle between the jet faking the τ decay products and the lepton. Hence the discriminating

([2]) In the following, the term "lepton", ℓ, refers to electrons and muons only.
([3]) In the following, reconstructed jets identified as hadronic τ decays are referred to as "τ candidates" or τ_h.

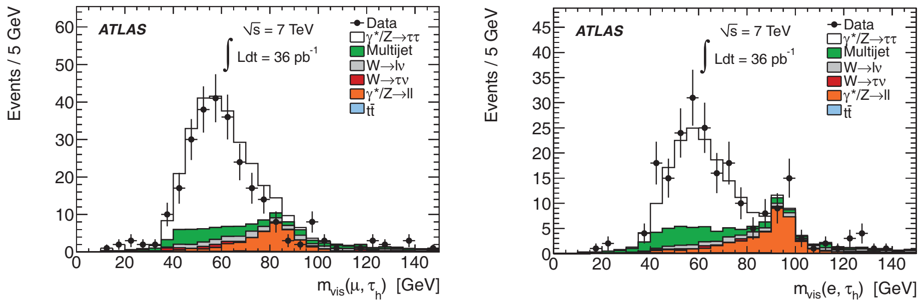

(a) $\tau_\mu \tau_h$ final state (b) $\tau_e \tau_h$ final state

Fig. 1. – The distributions of the visible mass of the combination of the τ candidate and the lepton are shown for the $\tau_\mu \tau_h$ (a) and $\tau_e \tau_h$ (b) final states. These distributions are shown after the full event selection, except for the visible mass cut [4].

variable $\sum \cos \Delta\phi$ is defined as

$$\sum \cos \Delta\phi = \cos\left(\phi(\ell) - \phi(E_T^{\text{miss}})\right) + \cos\left(\phi(\tau_{\text{h}}) - \phi(E_T^{\text{miss}})\right). \tag{2}$$

The variable $\sum \cos \Delta\phi$ is positive when the E_T^{miss} vector points towards the direction bisecting the decay products and is negative when it points away. The $W +$ jets backgrounds accumulate at negative $\sum \cos \Delta\phi$ whereas the $\gamma^*/Z \to \tau\tau$ distribution has an asymmetric tail extending into positive $\sum \cos \Delta\phi$ values, corresponding to events where the Z boson has higher p_T. Events are therefore selected by requiring $\sum \cos \Delta\phi > -0.15$.

The transverse mass, defined as

$$m_{\text{T}} = \sqrt{2\, p_{\text{T}}(\ell) \cdot E_T^{\text{miss}} \cdot \left(1 - \cos \Delta\phi(\ell, E_T^{\text{miss}})\right)}, \tag{3}$$

displays a Jacobian peak at the W boson mass for $W \to l\nu$ events, whereas $Z \to \tau\tau$ events cluster towards zero. In the present selection the transverse mass is required to be $m_{\text{T}} < 50$ GeV.

Additionally, any event with more than one muon or electron candidate is vetoed, which strongly suppresses background from $\gamma^*/Z \to \ell\ell +$ jets events, which can fake the $Z \to \tau\tau$ signature in the same way as $W \to l\nu$ events as well as with a lepton faking the τ signature.

Selected events are then required to have a visible mass in the range $35 < m_{\text{vis}} < 75$ GeV. This window is chosen to include the bulk of the signal, while avoiding background contamination from $Z \to \ell\ell$ decays. Finally, the chosen τ candidate and the chosen lepton are required to have opposite charges (OS) as expected from $Z \to \tau\tau$ decays. The visible mass distribution for the fully selected events in the $\tau_\mu \tau_{had}$ and $\tau_e \tau_{had}$ is shown in fig. 1. The purely kinematic requirements, defining the fiducial region for the

TABLE I. – *Expected number of events per process and number of events observed in data for an integrated luminosity of* $36\,\mathrm{pb}^{-1}$*, after the full selection. The background estimates have been obtained as described in sect.* **6**. *The quoted uncertainties are statistical only* [4].

	$\tau_\mu\tau_h$	$\tau_e\tau_h$
$\gamma^*/Z \to ll$	11.1 ± 0.5	6.9 ± 0.4
$W \to l\nu$	9.3 ± 0.7	4.8 ± 0.4
$W \to \tau\nu$	3.6 ± 0.8	1.5 ± 0.4
$t\bar{t}$	1.3 ± 0.1	1.02 ± 0.08
Diboson	0.28 ± 0.02	0.18 ± 0.01
Multijet	24 ± 6	23 ± 6
$\gamma^*/Z \to \tau\tau$	186 ± 2	98 ± 1
Total expected events	235 ± 6	135 ± 6
N_{obs}	213	151

cross-section measurement, can be summarised as

$\tau_\mu\tau_h$	final state: Muon $p_{\mathrm{T}} > 15\,\mathrm{GeV}$, $\lvert\eta\rvert < 2.4$ Tau $p_{\mathrm{T}} > 20\,\mathrm{GeV}$, $\lvert\eta\rvert < 2.47$, excluding $1.37 < \lvert\eta\rvert < 1.52$ Event $\Sigma \cos\Delta\phi > -0.15$, $m_{\mathrm{T}} < 50\,\mathrm{GeV}$, m_{vis} within [35, 75] GeV
$\tau_e\tau_h$	final state: Electron $E_T > 16\,\mathrm{GeV}$ $\lvert\eta\rvert < 2.47$, excluding $1.37 < \lvert\eta\rvert < 1.52$ Tau $p_{\mathrm{T}} > 20\,\mathrm{GeV}$ $\lvert\eta\rvert < 2.47$, excluding $1.37 < \lvert\eta\rvert < 1.52$ Event $\Sigma \cos\Delta\phi > -0.15$ $m_{\mathrm{T}} < 50\,\mathrm{GeV}$, m_{vis} within [35, 75] GeV

6. – Background estimation

In order to determine the purity of the selected $Z \to \tau\tau$ events and the $Z \to \tau\tau$ production cross-section, the number of background events passing the selection cuts must be estimated. The contributions from the $\gamma^*/Z \to ll$, $t\bar{t}$ and diboson backgrounds are taken from Monte Carlo simulations, while all other backgrounds are estimated using partially or fully data-driven methods.

The $W \to \ell\nu$ and $W \to \tau\nu$ are constrained with data by obtaining their normalization from a W-boson–enriched control region. This normalization corrects the Monte Carlo for an overestimate of the probability for quark and gluon jets produced in association with the W boson to be misidentified as hadronic τ decays.

The multijet background estimation is made by employing a data-driven method. A multijet enriched control region is constructed by requiring the two candidate τ decay products to have the same sign (SS). The ratios of events where the decay products have the opposite sign to those where they have the same sign $R_{\mathrm{OS/SS}}$ is then measured in a separate pair of control regions where the lepton isolation requirement is inverted. Electroweak backgrounds in all three control regions are subtracted using Monte Carlo simulations.

Table I shows the estimated number of background events per process and the expected number of signal events, as well as the total number of events observed in data

TABLE II. – *Relative statistical and systematic uncertainties in % on the $Z \to \tau\tau$ total cross-section measurement. The electron and muon efficiency terms include the lepton trigger, reconstruction, identification and isolation uncertainties, as described in ref.* [4].

Systematic uncertainty	$\tau_\mu\tau_h$	$\tau_e\tau_h$
Muon efficiency	3.8%	–
Muon resolution and energy scale	0.2%	–
Electron efficiency, resolution and charge misidentification	–	9.6%
τ_h identification efficiency	8.6%	8.6%
τ_h misidentification	1.1%	0.7%
Energy scale (e/τ/jets/E_T^{miss})	10%	11%
Multijet estimate method	0.8%	2%
W normalization factor	0.1%	0.2%
Object quality cuts	1.9%	1.9%
pile-up description in simulation	0.4%	0.4%
Theoret. cross-section	0.2%	0.1%
A_Z systematics	3%	3%
Total Systematic uncertainty	15%	17%
Statistical uncertainty	9.8%	12%
Luminosity	3.4%	3.4%

after the full selection. Further details on the background estimation methods can be found in ref. [4].

7. – Systematic uncertainties

Several possible sources of systematic uncertainty affect the cross-section measurement as uncertainties on the background estimation, on the signal yield, on the extrapolation of the fiducial cross-section to the total one and on the luminosity. A summary of systematic uncertainties can be found in table II.

Uncertainties on the background estimation come from uncertainties in the Monte Carlo predictions and from the assumptions at the basis of the methods used to perform the data-driven background estimates. Uncertainties on the Monte Carlo predictions are estimated either as statistical and systematic uncertainties in data-driven methods used ATLAS-wide to check or correct the Monte Carlo predictions or by varying the simulation conditions. Efficiencies of lepton trigger, identification and isolation fall in the first category, as well as rates of misidentification of electrons and jets as τ candidates, whereas uncertainties on the τ energy scale and identification efficiency fall in the second. The systematic uncertainty due to the multijet background estimate method is assessed by studying the dependence of the $R_{\text{OS/SS}}$ on the isolation variables cuts. The uncertainty on the W+jets background estimation method is dominated by the statistical uncertainty on the calculation of the normalization factor in the W control region.

The uncertainty on the correction factor C_Z is entirely due to the uncertainty in the Monte Carlo prediction for signal, and was assessed as in the case of background estimation explained above.

The theoretical uncertainty on the geometric and kinematic acceptance factor A_Z is dominated by the limited knowledge of the proton parton distribution functions (PDFs)

TABLE III. – *The components of the $Z \to \tau\tau$ cross-section calculations for each final state. For $N_{\rm obs} - N_{\rm bkg}$ the first uncertainty is statistical and the second systematic. For all other values the total error is given* [4].

	$\tau_\mu\tau_h$	$\tau_e\tau_h$
$N_{\rm obs}$	213	151
$N_{\rm obs} - N_{\rm bkg}$	$164 \pm 16 \pm 4$	$114 \pm 14 \pm 3$
A_Z	0.117 ± 0.004	0.101 ± 0.003
C_Z	0.20 ± 0.03	0.12 ± 0.02
B	0.2250 ± 0.0009	0.2313 ± 0.0009
$\mathcal{L}$	$35.5 \pm 1.2\,\mathrm{pb}^{-1}$	$35.7 \pm 1.2\,\mathrm{pb}^{-1}$

and the modeling of the Z boson production at the LHC. These are assessed by considering PDFs errors and varying sets, as well as changing the Monte Carlo generator used for the signal sample. The uncertainty on the luminosity is taken to be 3.4% [8]. A number of other sources, such as the uncertainty due to the object quality requirements on τ candidates and on jets, are also evaluated but have a small impact on the total uncertainty. The largest systematic uncertainties are due to the τ energy scale and identification efficiencies.

8. – Results

The inputs to the cross-section calculation are shown in table III, whereas the final results, obtained with the method described in sect. **4**, are shown in table IV and fig. 2. The results for the $\tau_e\tau_\mu$ and $\tau_\mu\tau_\mu$ channels and the combination of the four measurements described in ref. [4] are shown as well in fig. 2.

It can be seen that there is a good agreement among $Z \to \tau\tau$ channels, with the other $Z \to ll$ channels at ATLAS [9]. The gray band in fig. 2 represents the NNLO theory expectation of $0.96 \pm 0.05\,\mathrm{nb}$, with which is found to be in agreement with the measurements. The obtained result is compatible with the $Z \to \tau\tau$ cross-section in four final states published recently by the CMS Collaboration [10], 1.00 ± 0.05 (stat) $\pm$ 0.08 (syst) $\pm\, 0.04$ (lumi) nb, in a mass window of [60, 120] GeV.

TABLE IV. – *The production cross-section times branching fraction for the $Z \to \tau\tau$ process as measured for the two semileptonic channels. For the fiducial cross-sections the measurements include also the branching fraction of the τ to its decay products. The first error is statistical, the second systematic and the third comes from the luminosity* [4].

Final state	Fiducial cross-section (pb)
$\tau_\mu\tau_h$	$23 \pm 2 \pm 3 \pm 1$
$\tau_e\tau_h$	$27 \pm 3 \pm 5 \pm 1$
Final state	**Total cross-section ([66, 116] GeV) (nb)**
$\tau_\mu\tau_h$	$0.86 \pm 0.08 \pm 0.12 \pm 0.03$
$\tau_e\tau_h$	$1.14 \pm 0.14 \pm 0.20 \pm 0.04$

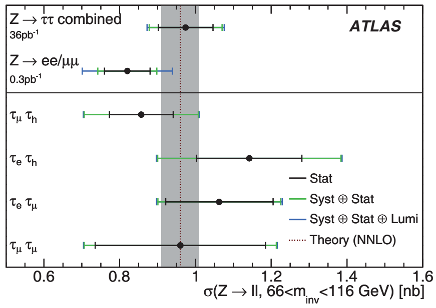

Fig. 2. – The individual cross-section measurements by final state, and the combined result. The $Z \to \ell\ell$ combined cross-section measured by ATLAS in the $Z \to \mu\mu$ and $Z \to ee$ final states is also shown for comparison. The gray band indicates the uncertainty on the NNLO cross-section prediction [4].

The presented analysis is a pioneering one for di-tau studies at ATLAS. It allowed for a better understanding of tau performance. Methods for data-driven estimates of the background were designed and tested in this context, that will be fundamental in other physics channels including taus.

* * *

I thank first of all the LHC and ATLAS teams, for the operation of the LHC and of the ATLAS detector, as well as the support of the staff of the institutions supporting ATLAS, in particular of the INFN. I would really like to thank all of the ATLAS $Z \to \tau\tau$ analysis group for the work together on this measurement. In particular I thank for their help and support E. Coniavitis, A. Kaczmarska and S. Kuhen, as well as my supervisors from INFN and Università degli Studi di Milano, D. Cavalli and A. Andreazza. I thank the Società Italiana di Fisica for the opportunity of giving this communication and for the prize as best communication of the Nuclear and Subnuclear Physics session at the Congresso Nazionale 2011, in particular the president Luisa Cifarelli and Guido Tonelli, president of the Nuclear and Subnuclear Physics session.

REFERENCES

[1] Nakamura K. *et al.*, *J. Phys. G*, **37** (2010) .
[2] The ATLAS Collaboration, *JINST*, **3** (2008) .
[3] Lyndon Evans and Philip Bryant, *JINST*, **3** (2008) .
[4] ATLAS Collaboration, *Phys. Rev. D*, **84** (2011) 11.
[5] The ATLAS Collaboration, ATLAS-CONF-2010-03.
[6] Agostinelli S. *et al.*, *Nucl. Instrum. Methods A*, **506** (2003) 250.
[7] The ATLAS Collaboration, *Eur. Phys. J. C*, **70** (2010) 823.
[8] The ATLAS Collaboration, ATLAS-CONF-2011-011.
[9] The ATLAS Collaboration, *JHEP*, **12** (2010) 060.
[10] The CMS Collaboration, arXiv:1104.1617[hep-ex].